AIP | Journal of Applied Physics

Method of evaluating thermal diffusivity near lossy boundaries as an alternative to the Parker method

Harry I. Ringermacher

Citation: J. Appl. Phys. **113**, 154903 (2013); doi: 10.1063/1.4800886
View online: http://dx.doi.org/10.1063/1.4800886
View Table of Contents: http://jap.aip.org/resource/1/JAPIAU/v113/i15
Published by the AIP Publishing LLC.

JOURNAL OF APPLIED PHYSICS **113**, 154903 (2013)

Method of evaluating thermal diffusivity near lossy boundaries as an alternative to the Parker method

Harry I. Ringermacher
General Electric Global Research Center 1 Research Circle, Niskayuna, New York 12309, USA

(Received 14 February 2013; accepted 25 March 2013; published online 17 April 2013)

We describe an analysis of a flash thermographic method to measure thermal diffusivity that is particularly insensitive to heat loss mechanisms near thermal boundaries. This approach is an alternative to the "Parker method" which requires that a plate-like region subject to a uniform energy flux must reach a maximum constant temperature in order to obtain an accurate measurement of thermal diffusivity at the half-temperature point in time. The present approach relies on evaluating another unique point, the inflection point, of the same back-side thermal response curve as Parker's or, from the front side, using a contrast versus time curve in the sample region of interest. This inflection point occurs so early in the response history that little heat loss, for example, near heat-sink boundaries or surface convection, is expressed. Since the method is insensitive to the achieved temperature, it is also insensitive to surface emissivity variations. © *2013 AIP Publishing LLC* [http://dx.doi.org/10.1063/1.4800886]

I. INTRODUCTION

Parker *et al.*[1] were the first to describe a flash thermographic method for the measurement of thermal diffusivity. Winfree *et al.*[2] describe improvements in this method for non-destructive evaluation using infrared (IR) cameras rather than a point-wise detector. Other techniques are described in Maldague.[3] Nevertheless, the Parker method predominates. The typical Parker method system requires the fabrication of a "standard plate specimen" for flash evaluation. The back surface temperature is monitored following a front-side optical flash and the time at the half-temperature point is used to calculate the thermal diffusivity for a known thickness. Industrial applications have placed new demands on measurement of thermal properties. In particular, *in-situ* measurement is often the only option. Industrial components such as engine blades and vanes and other parts may have spatially varying thermal properties as well as varying thickness in a complex structure. An example would be a hollow engine blade with an internal rib structure. It might be desirable to measure wall thickness or thermal diffusivity near a rib junction. The Parker method would fail in this location for two reasons: (1) the back is inaccessible and (2) there is significant heat loss to the rib. The surface temperature cannot achieve a reliable maximum.

In this paper, we will present an alternative analysis that is more tolerant of heat loss near such boundaries. This approach relies on evaluating another unique point, the inflection point, of the same back thermal response curve as Parker's or, from the front side, using a contrast versus time curve in the sample region of interest. The author first utilized the contrast inflection point for the non-destructive evaluation of flaws in materials.[4,5] This inflection point occurs so early in the response history that little heat loss, for example, near heat-sink boundaries or surface convection, is expressed. Temperature contrast is here defined as the temperature-time history at a point on the finite sample region minus the temperature-time history of a properly normalized infinite half-space. When observing the response from the same side as the flash, a contrast must be evaluated to create an inflection point. The temperature response observed from the back has a natural inflection point and does not need a "reference curve." In order to apply this approach, one must assume the sample to be "plate-like" and subject to 1-dimensional (1-d) heat flow. The volume above a circular insulating gap or "delamination" can be treated as "plate-like" flaw. A flashlamp is used to create a flux at the surface and the same surface or back surface (in the case of an actual plate) is monitored by an IR sensor or camera. If the plate thickness is known, the thermal diffusivity can be extracted or vice-versa. The method could then determine, quite precisely, the flaw depth (plate thickness) if the diffusivity is known or vice-versa. Prior to the work of Ref. 4, attempts to determine flaw depth were correlated to peak contrast times.[6,7] However, it was pointed out that the contrast peak time is dominated by flaw dimension effects since the heat must flow around the "plate" significantly distorting the depth evaluation. The utilization of the contrast inflection point corrected this problem because of the relative insensitivity of the inflection point to heat loss at the flaw edge and thus flaw diameter. Recent work by Almond and Pickering[8] has addressed the influence of heat flow around a "plate-like" flaw and thus helped to clarify the sensitivity to flaw detection at varying diameter/depth aspect ratios. Their work has also helped elucidate the contrast inflection method as will be described below.

II. THEORY OF THE METHOD

A. Through-transmission response

We begin by considering the same situation as Parker, namely, a "through-transmission" response with observation from the back.

For a constant optical flux of length τ impinging on an absorbing surface of a plate of thickness l at $x = 0$, a heat flux, F J/m^2/s, diffuses from the surface into the bulk. For this flux, the temperature rise for $t > \tau$ at the back surface at $x = l$ is given by[10]

$$T(t) = \frac{J_0}{\rho c l} - \frac{2Fl}{\pi^2 K}\left(\sum_{n=1}^{\infty}(-1)^n \frac{e^{-\frac{n^2 t}{T_c}}}{n^2}\left(1 - e^{-\frac{n^2\tau}{T_c}}\right)\right), \tag{1}$$

where the thermal diffusivity is $\alpha = K/(\rho c)\,\mathrm{m}^2/\mathrm{s}$ and the "characteristic time" is

$$T_c = l^2/(\pi^2\alpha). \tag{2}$$

In the limit as $\tau \to 0$, this expression simplifies

$$T(t) = \frac{J_0}{\rho c l}\left(1 + 2\sum_{n=1}^{\infty}(-1)^n e^{-\frac{n^2 t}{T_c}}\right). \tag{3}$$

K, c, and ρ are thermal conductivity, specific heat, and density. Expression (3) is identical to Parker's Eq. (2). The quantity $J_0/(\rho c l)$ is the plate temperature limit as $t \to \infty$.

We can find the inflection point for Eq. (3) by taking the second derivative with respect to time and setting it to zero, then solving for the time, $t = t_{infl}$.

The equation to be solved is

$$\sum_{n=1}^{\infty}(-1)^n n^4 e^{-n^2 p} = 0. \tag{4}$$

This equation can be solved numerically for $p \equiv t_{infl}/T_C$. We find

$$t_{infl} = 0.9055\,T_C. \tag{5}$$

This compares to Parker's "half-amplitude time"

$$t_{1/2} \equiv 1.38\,T_C. \tag{6}$$

We see that the inflection time occurs significantly earlier than the half-max temperature time and is independent of the need to obtain a maximum temperature altogether. A plot of a typical through-transmission curve with its derivative maximum indicating the inflection point is shown in Fig. 1. Thus, if the inflection time is found from the temperature-time curve in through-transmission, the characteristic time is determined. Then, either the thickness or thermal diffusivity can be found if the other is known.

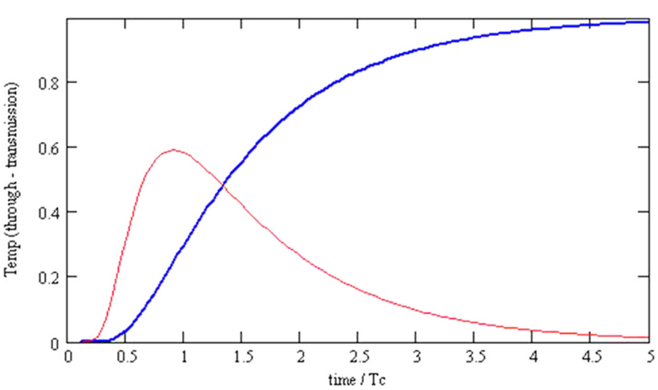

FIG. 1. Back-side plate response to a short input pulse (upper). Derivative of the plate response is shown to indicate a peak at the inflection time of Eq. (5). Time is in units of the characteristic time.

A question arises as to how well the above 1-d inflection point expression applies for more realistic 2-d axisymmetric heat flow near boundaries. This has been modeled using finite elements[4] for various plate radius/depth aspect ratios for the front-side contrast measurement case and applies equally well to the above back-side case. Results indicate that the inflection point is stable to a radius/depth ratio of at least 1.25. This result is measured at the plate center. For example, for a unit depth, and a plate radius of 1.25 depths, the center depth will indicate very nearly 1. As one approaches the plate edge, the depth error increases. A similar result applies for diffusivity but diffusivity error is twice the depth error as one can see from Eq. (2) for fixed inflection time. This will be addressed in more detail after a discussion of the front-side contrast response in Sec. II B.

B. Same-side response

We first address the infinite half-space surface response to an optical input flux. The temperature at the front surface, $x = 0$, of an infinite half-space for times $t > \tau$, where τ is the width of a short rectangular heat flux into the surface, is given by[10]

$$T_0(t) = \frac{2F}{\sqrt{\pi K \rho c}}\left(\sqrt{t} - \sqrt{t - \tau}\right). \tag{7}$$

The temperature seen at the front surface of the plate at $x = l$ for times $t > \tau$, analyzed similarly to the back case is given by

$$T(t) = \frac{J_0}{\rho c l} - \frac{2Fl}{\pi^2 K}\left(\sum_{n=1}^{\infty}\frac{e^{-\frac{n^2 t}{T_c}}}{n^2}\left(1 - e^{-\frac{n^2\tau}{T_c}}\right)\right). \tag{8}$$

In the limit as $\tau \to 0$, Eqs. (7) and (8), respectively, simplify

$$T_0(t) = \frac{J_0}{E\sqrt{\pi t}} \tag{9}$$

$$T(t) = \frac{J_0}{\rho c l}\left(1 + 2\sum_{n=1}^{\infty} e^{-\frac{n^2 t}{T_c}}\right). \tag{10}$$

$J_0 = F\tau$ is the energy intensity into the surface and $E = \sqrt{K\rho c}$ is the thermal effusivity.

K, ρ, and c are, respectively, the thermal conductivity, density, and specific heat. This solution is the same as used in Cramer *et al.*,[2] mentioned earlier. It is essential for accuracy that short ($\tau \ll T_c$), rectangular pulses, rather than exponentially decaying pulses, are used. Laser pulses are typically used for accurate measurements, but electronically quenched flash-lamps can also be used.[11]

Contrast is defined from Eqs. (9) and (10) simply as

$$C(t) = T(t) - T_0(t) = \frac{J_0}{\rho c l}\left(1 + 2\sum_{n=1}^{\infty} e^{-\frac{n^2 t}{T_c}}\right) - \frac{J_0}{E\sqrt{\pi t}}. \tag{11}$$

The inflection point for the same-side contrast, Eq. (11) can be found similarly to the approach of Eqs. (4) and (5)

$$t_{infl} = 4(0.9055)\,T_C = 3.622\ T_C. \tag{12}$$

The factor of four arises fundamentally from a "round trip" doubling, $2l$, of the thermalization path. The thermalization time is proportional to the path length squared. Equations (5) and (12), the primary results of this paper, have been employed extensively for nondestructive testing of complex shaped components with lossy boundaries and single-side access such as hollow aircraft engine and power turbine blades.[12]

Almond and Pickering,[8] have recently revisited and extended earlier work[9] describing an equivalent solution, Eq. (13) to the same-side response as our Eq. (10)

$$T(t) = \frac{J_0}{E\sqrt{\pi t}}\left(1 + 2\sum_{n=1}^{\infty} e^{-\frac{n^2 l^2}{\alpha t}}\right). \tag{13}$$

Almond's presentation elucidates our definition of contrast, Eq. (11), and further studies heat flow near boundaries. The lead term is the half-space solution, Eq. (9). If we subtract the half-space response from the plate solution, Eq. (13), we are left with a "natural" definition of contrast, the second term of Eq. (13), fully equivalent to our definition, $C(t)$, Eq. (11). In order to use same-side contrast in a practical manner, one need not actually measure a physical half-space reference temperature. A properly normalized ideal response, Eq. (9), can be used for this evaluation and subtracted from the measured surface temperature data. This is described in earlier work.[13,14] The inflection point is then located and Eq. (12) used to calculate either diffusivity or sample thickness. Shepard *et al.*[15] have used a logarithmic derivative evaluation of flaw data, but not inflection point imaging as described above. We have not analyzed the logarithmic inflection point time to compare with our contrast inflection point. However, Maldague[3] refers to a "transit time" at which point a same-side thermal response curve deviates from its half-space, $1/\sqrt{t}$, behavior. This gives an equivalent time. Its value is stated as

$$t_T \sim \frac{0.36\,l^2}{\alpha} \approx 3.6\,T_c.$$

This agrees closely with our exact inflection point time, Eq. (12), suggesting that the "transit time" is, in fact, the inflection point time.

We shall now address the accuracy limits of this approach in more realistic 2-d heat flow. Almond and Pickering[8] have addressed this extensively in relation to peak contrast time, but we shall look only at contrast inflection time modeling relevant to the present work.

III. STABILITY OF THE CONTRAST INFLECTION POINT

The stability of the contrast inflection point was first studied by the author[4] using finite element methods. Those results indicated the inflection point was stable with 2-d heat flow, located between $3\,T_c - 4\,T_c$ compared to the 1-d result of about $3.6\,T_c$. A later more precise 2-d study is shown below. Figure 2 is a drawing of a notched nickel super alloy plate used to measure thermal response to flash thermography. The notches have varying aspect ratios (half-width/depth) relative to the plate-surface, as dimensions indicate. The notch specimen response was first modeled with an input pulse applied on the flat side with same-side response monitoring. Figure 3 shows the results of this study. The curves plot the depth of the notch, obtained from the inflection time, as a function of position across the notch. Superimposed is a cross section of the notch as a solid line. For each aspect-ratio response curve (indicated by the number below it), a dotted line indicates the center of the corresponding notch (with an imaginary reflected boundary on its left—just as the one on the right). Lengths are normalized to the notch depth. Aspect ratios 10, 5, and 2.5 show nearly overlaying curves. For these aspect ratios, the error in the 1-d formula (12) is 0.7%. For an aspect ratio of 1.25, that error increases to 5%. As the aspect ratio continues to decrease, the error appears to approach a limit of about 15%. However, as Almond demonstrates, the surface signal decreases rapidly as our aspect ratio shrinks below 1 (2 in the Almond paper for comparison), so the flaw image considerably weakens. Nevertheless, the contrast inflection time

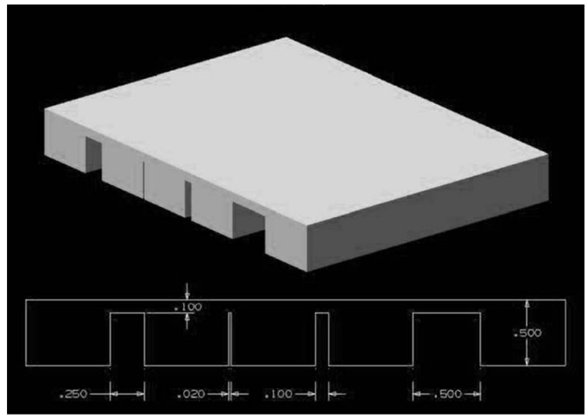

FIG. 2. Notched nickel-alloy plate with notches of varying aspect ratio (half-width/depth). Depth of notch from surface is constant at 0.100 in.

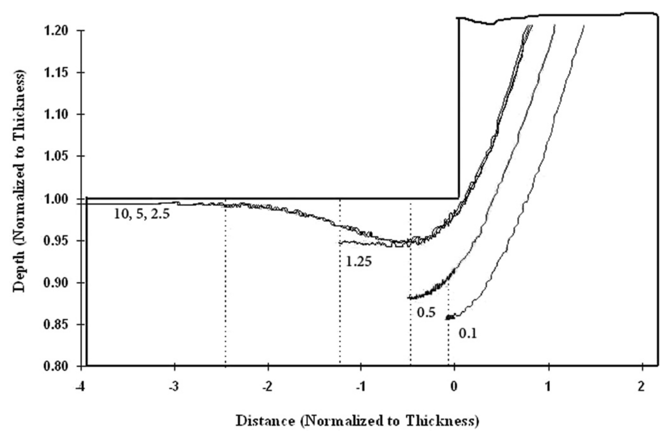

FIG. 3. Modeling results of notched plate inflection point imaging showing normalized depth vs. normalized position along notch. Dotted lines indicate notch center for each aspect ratio curve. Curve ends at notch center and is symmetric about it.

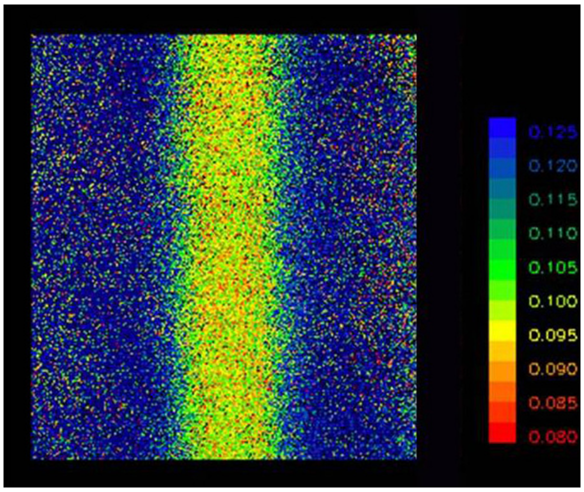

FIG. 4. Flash-thermography inflection point image of 1.25 aspect ratio notch of plate of Fig. 2 (left-most notch). Color bar indicates notch depth below the surface in inches. Insufficient time data were taken to acquire a correct background plate thickness so that dimension is meaningless.

displays relatively small depth error across the notch to very near the boundary. This is consistent with what has been observed.

To verify this conclusion, the notched plate was imaged using inflection point mapping as described above. This work was actually performed in 1998 and, at the time, unpublished. Speedotron type 105, 2-cable, lamps were used. These are high speed units with FWHM of 1.5 ms, each powered by 4.8 kJ supplies and are still available. Lamp quenching (providing a sharp rectangular optical pulse), often used for high resolution work today, was not necessary under these conditions. The camera used was a Amber/Raytheon, Radiance HS, a Stirling-cooled focal plane array (256 × 256 pixels) IR camera at 3–5 μm wavelength. It is important to choose a camera frame rate that permits adequate time resolution of the inflection point, thus, determining the depth error of the data. The speed chosen was 100 FPS with a 1.5 ms integration time. This speed provided time resolution within the calculated error expectations. The same-side inflection time for this 0.1 in. thick nickel alloy (diffusivity = 0.028 cm^2/s) is 0.85 s according to Eqs. (2) and (12). The thermal "depth image" of the 1.25 aspect notch is shown in Fig. 4. The depth image is a same-side flash thermography image taken at the top of the plate. Rather than mapping the temperature in this image, we map the same-side contrast inflection point. The color-bar on the right indicates the notch depth in inches. A depth profile across the image, shown in Fig. 5, shows a "flat-top" inflection time response (lower curve centered at $X = 0.55$) compared to the Gaussian temperature profile of the notch. The "y-axis" is the notch depth for this curve. The measured notch depth is 0.1 in. and the imaged value is 0.097 in., close to the predicted 0.095 in. shown in the profile calculation of Fig. 3. In fact, the profiles are similar. Thus, the contrast inflection method produces sharper images than traditional thermal imaging.

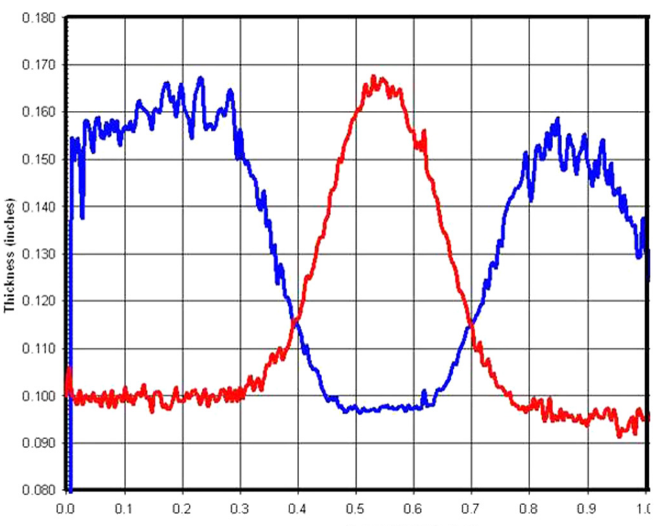

FIG. 5. Inflection point data profile across image of Fig. 4 (flat-bottom curve at center) compared to temperature profile across same image (Gaussian curve at center). The thickness scale measures depth of notch and is accurate only in the notch region (see Fig. 4). The thermal response has arbitrary scale.

IV. CONCLUSIONS

We have shown that use of contrast inflection time imaging is relatively insensitive to heat loss at boundaries. Thus, the method can be used to measure the thermal diffusivity or depth of plate-like regions in prepared samples or actual components to accuracies of 1%–15%, depending on the aspect ratios of the region. We have also shown that this type of imaging will produce sharper images of "flaws" than traditional temperature mapping. Inflection point mapping permits evaluation of depth of flaws and thicknesses/diffusivities without the need for separately imaging standards representative of the material or for comparative measurements on the same material.

ACKNOWLEDGMENTS

I wish to thank Bryon E. Knight and Donald R. Howard at the GE Global Research Center for supporting my efforts over these many years and for making this type of infra-red NDT evaluation actually happen and moving it onto the industrial floor.

[1]W. J. Parker, R. J. Jenkins, C. P. Butler, and G. L. Abbot, J. Appl. Phys. **32**, 1679 (1961).
[2]K. E. Cramer, W. P. Winfree, E. R. Generazio, R. Bhat, and S. Fox, *Review of Progress in Quantitative Nondestructive Evaluation* (Plenum Press, 1993), Vol. 12, p. 1305.
[3]X. V. Maldague, *Theory and Practice of Infrared Technology for Nondestructive Testing* (John Wiley & Sons, 2001).
[4]H. I. Ringermacher, D. J. Mayton, D. R. Howard, and B. N. Cassenti, *Review of Progress in Quantitative Nondestructive Evaluation* (Plenum Press, 1998), Vol. 17, p. 425.
[5]H. I. Ringermacher *et al.*, "Nondestructive testing: Transient depth thermography," U.S. patent 5,711,603 (1998).
[6]L. D. Favro, P. K. Kuo, and R. L. Thomas, *Review of Progress in QNDE* (Plenum Press, 1994), Vol. 13, p. 395.
[7]V. P. Vavilov, E. Grinzato, P. G. Bison, S. Marinetti, and C. Bressan, Mater. Eval. **54**, 604 (1996).
[8]D. P. Almond and S. G. Pickering, J. Appl. Phys. **111**, 093510 (2012).
[9]S. K. Lau and D. P. Almond, J. Phys. D: Appl. Phys. **24**, 428 (1991).

[10]H. S. Carlslaw and J. C. Jaeger, *Conduction of Heat in Solids*, 2nd ed. (Oxford University Press, 1959).
[11]H. Ringermacher, D. R. Howard, and R. J. Filkins, *Review of Progress in Quantitative Nondestructive Evaluation* (AIP, 2004), Vol. 23, p. 477.
[12]H. Ringermacher, D. Howard, and B. Knight, *Review of Progress in Quantitative Nondestructive Evaluation* (AIP, 2006), Vol. 25, p. 523.
[13]H. I. Ringermacher and D. R. Howard, *Review of Progress in Quantitative Nondestructive Evaluation* (AIP, 2001), Vol. 20, p. 487.
[14]H. I. Ringermacher *et al*., "Method and apparatus for thermographic nondestructive evaluation of an object," U.S. patent 7,549,789 (2006).
[15]S. M. Shepard, J. R. Lhota, B. A. Rubadeaux, D. Wang, and T. Ahmed, *Review of Progress in Quantitative Nondestructive Evaluation* (AIP, 2003), Vol. 22, p. 1270.